OSH

UCID- 16986-86-2

LAWRENCE LIVERMORE NATIONAL LABORATORY
OIL SHALE PROJECT QUARTERLY REPORT

APRIL - JUNE 1986

A. E. Lewis, Editor

For
U.S. Department of Energy
Office of Fossil Energy
Morgantown Energy Technology Center
Laramie Project Office
Laramie, Wyoming

July 1986

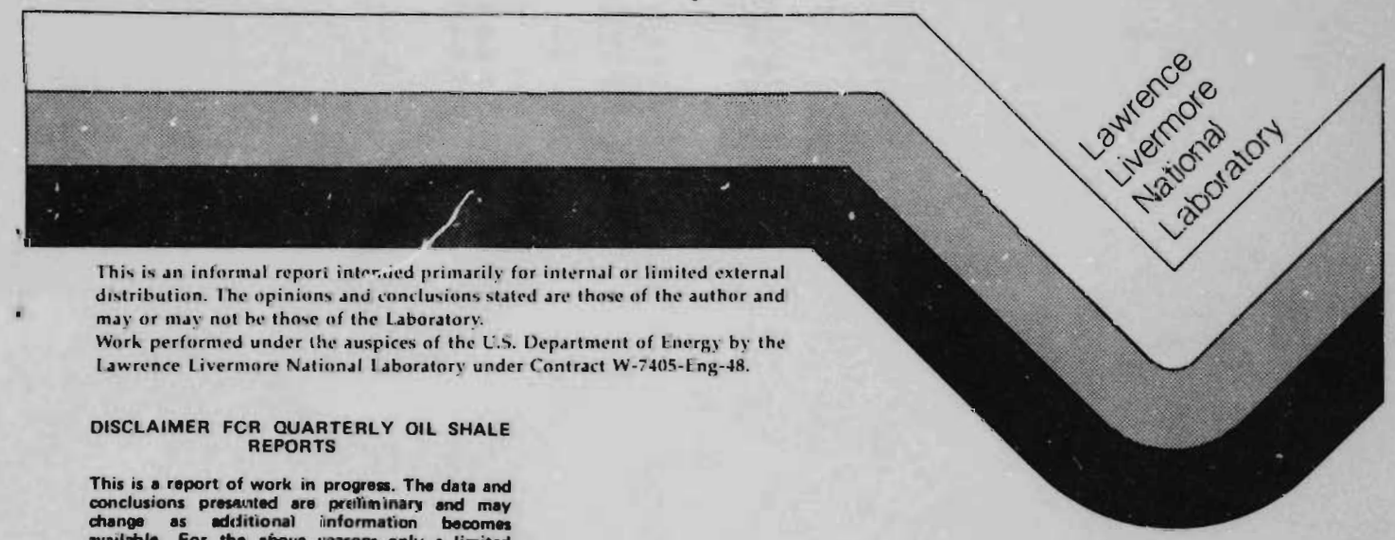

DISCLAIMER

Printed in the United States of America
Available from
National Technical Information Service
U.S. Department of Commerce
5285 Port Royal Road
Springfield, VA 22161
Price: Printed Copy $; Microfiche $4.50

Page Range	Domestic Price	Page Range	Domestic Price
001-025	$ 7.00	326-350	$ 26.50
026-050	8.50	351-375	28.00
051-075	10.00	376-400	29.50
076-100	11.50	401-426	31.00
101-125	13.00	427-450	32.50
126-150	14.50	451-475	34.00
151-175	16.00	476-500	35.50
176-200	17.50	501-525	37.00
201-225	19.00	526-550	38.50
226-250	20.50	551-575	40.00
251-275	22.00	576-600	41.50
276-300	23.50	601-up[1]	
301-325	25.00		

[1]Add 1.50 for each additional 25 page increment, or portion thereof from 601 pages up.

OIL SHALE QUARTERLY REPORT

April - June 1986

Contents

I. ENTHALPY RELATIONS FOR OIL SHALE

New relations have been obtained for the heat capacities of shale oil, and the mineral, bound water, and organic fractions of oil shale. New values have been obtained for the heat of bound water dehydration and the heat of pyrolysis. Although developed for Green River shale, all but the heat of pyrolysis can be modified easily for Eastern shale without additional calorimetric data. Table 1 summarizes the new recommended relations which fit the existing calorimetric data on raw, spent, and burned shale very well.

"Handbook" enthalpy values of the minerals present in typical Green River Formation oil shale (raw, spent, and burned composite) were added by weight fraction and fitted to obtain the heat capacity of the mineral portion of oil shale as a quadratic in temperature. This is very insensitive to expected variations in Green River shale mineral composition, including those occurring in retorting processes.

Hydrated minerals are treated as the dehydrated mineral, included in the mineral fraction above, plus a separate component called bound water with its own heat capacity, heat of dehydration, and extent of vaporization dependence on temperature. The heat capacity was estimated by comparing the heat capacities of the hydrated and dehydrated forms of several minerals. The heat of dehydration was taken to be that measured for analcime (Johnson et al., Fuel, 1975). The temperature range of dehydration was from previous LLNL work.

Shale organic constituents (kerogen and char of various compositions) were treated based on a correlation established over a wide temperature range between the heat capacities of several model organic compounds and their

Table 1. Recommended heat capacity and heat of reaction relations for Green River oil shale. Here T is temperature [K], C is heat capacity [kJ/kg K], ΔH is reaction heat [kJ/kg reactant], X_H is the mass fraction of hydrogen in a compound, and X_v is the fraction of initial bound water which has vaporized.

C_{oil}		$= -2.548 + 0.0182T - 1.38 \times 10^{-5}T^2$
$C_{dry\ mineral}$		$= 0.3998 + 1.6675 \times 10^{-3}T - 8.395 \times 10^{-7}T^2$
$C_{bound\ water}$		$= 1.73 + 2.1 \times 10^{-3}T$
X_v		$= 0$ for $T<393$, $(T-393)/240$ for $393<T<633$, 1.0 for $T>633$
$\Delta H_{bw \rightarrow H_2O\ vapor}$		$= 2555.$
$C_{organic\ in\ shale}$		$= X_H C_H + (1-X_H)C_c$
where	C_H	$= 4.482 + 0.017066T$
	C_c	$= -0.269 + 3.889 \times 10^{-3}T - 1.8447 \times 10^{-6}T^2$
	X_H	$= 0.1036$ for Green River kerogen,
		$= 0.0773$ for Eastern kerogen,
		$= 0.0318$ for Green River Fischer assay char
		$= 0.0465$ for Green River rapid heating char
$\Delta H_{kerogen \rightarrow pyrolysis\ products}$		$= 410$

hydrogen mass fractions (see Figs. 1-2). The nonhydrogen heat capacity contribution was taken to be the heat capacity of graphite. The hydrogen heat capacity contribution and its temperature dependence was found from the above correlation. The heat capacity of compounds such as kerogen or char, with a known hydrogen mass fraction, is the weighted sum of these two contributions. This correlation is limited to compounds with less than 10% N and O content.

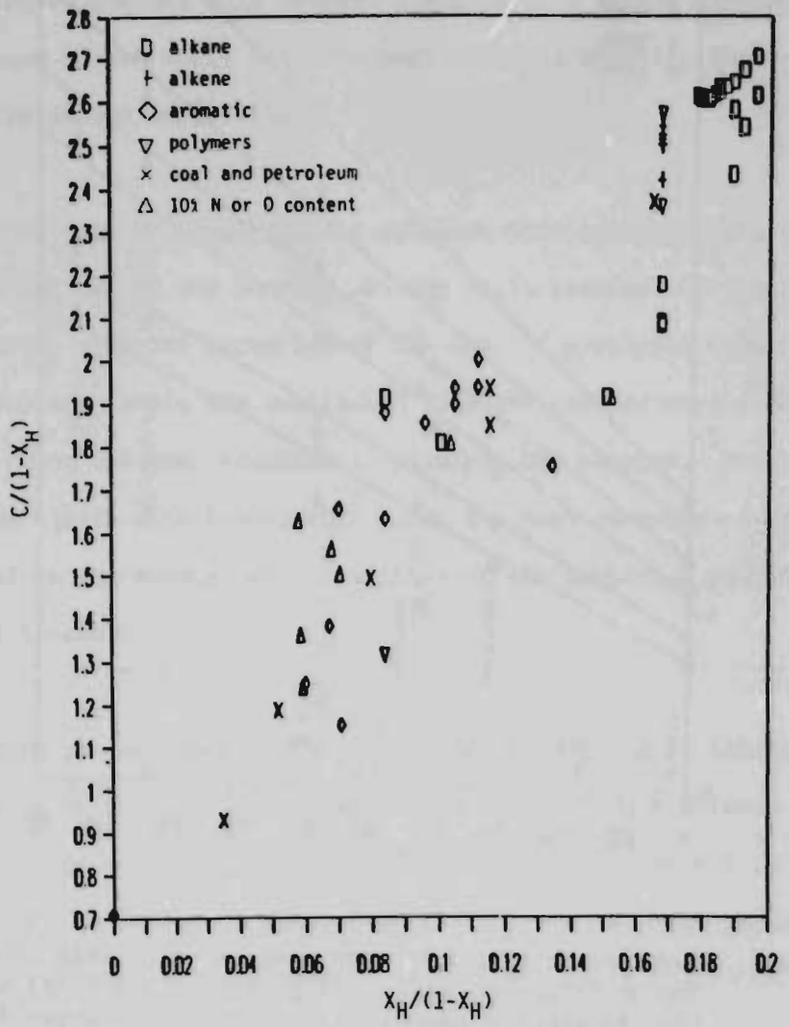

Figure 1. Organic (<10% non-HC) heat capacities at 25°C. If heat capacity could be described by $C=X_H C_H+(1-X_H)C_C$, then the above plot of values should produce a straight line with slope C_H and intercept C_C. Here X_H is the mass fraction of hydrogen in the compound, C_H is the heat capacity contribution from hydrogen, and C_C is the heat capacity contribution from non-hydrogen elements. The latter turns out to be very close to the heat capacity of graphite.

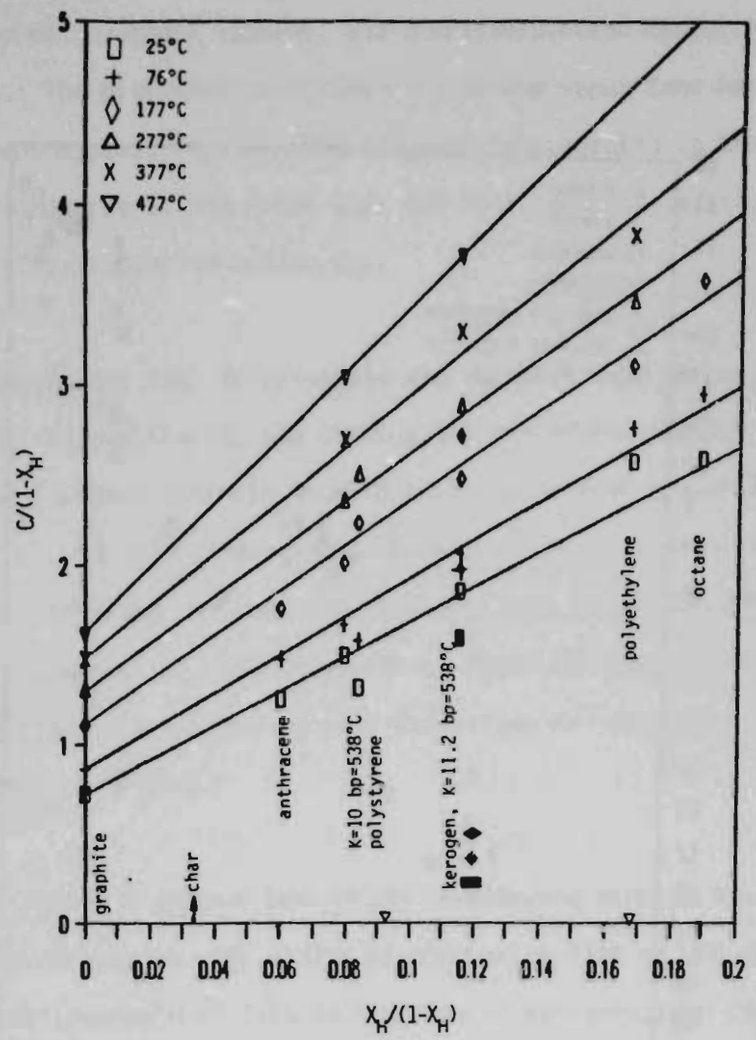

Figure 2. Model compound and kerogen heat capacity data plotted as though $C=X_H C_H+(1-X_H)C_C$. Aliphatic/aromatic characterization factor and average boiling point are shown for petroleum fractions. The intercept at each temperature is the value of the heat capacity for graphite, C_C. The slopes of the lines are fitted through the data and represent the heat capacity contribution of hydrogen, C_H.

The heat capacity relation for shale oil is based on the liquid and vapor enthalpies of a petroleum fraction which has the same specific gravity, mean boiling point, hydrogen content, and characterization factor as Fischer assay shale oil. The distribution between liquid and vapor (and hence the weighting of those enthalpies) changes with temperature according to the simulated distillation curve of the shale oil. The heat capacity relation thus contains the heat of vaporization implicitly.

The value for heat of pyrolysis was obtained from enthalpy data for five shales by first estimating and summing all the heats required during the actual experiments, with the exception of the heat of pyrolysis (see Fig. 3). This estimate for each shale was subtracted from the post-pyrolysis data, with the difference being the heat required to pyrolyze the kerogen. The heat of pyrolysis varies little with temperature since the heat capacity of kerogen is almost identical to the summed heat capacities of the pyrolysis products over temperatures of interest.

The relations we have been using in modeling studies up to this time were obtained by Carley at LLNL (1975) by regression fits of the available data. The main disadvantage of this approach is in extrapolating these fits to higher temperatures or different shale compositions such as high bound water content or Eastern minerals and kerogen. The new relations should be more accurate at higher temperatures and can be easily applied to shales of different composition.

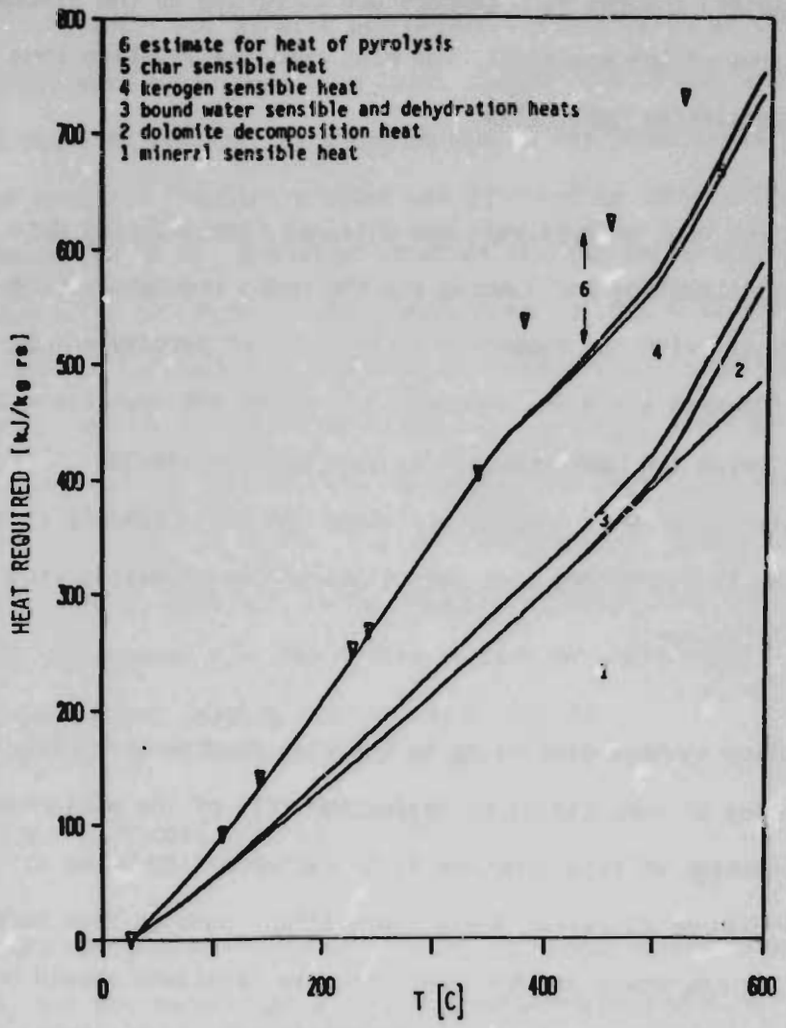

Figure 3. Measured (▽, Wise) and predicted cumulative heat requirements for 34.3 gpt shale. Most of the pyrolysis occurred between 340-370°C for these experiments. Above 370°C, the difference between data and top predicted line is the estimate for heat of pyrolysis, for this experiment.

II. CHEMICAL REACTION MODELING

We have completed the analysis of our experimental data for combustion of residual organic carbon in Colorado oil shale that has undergone rapid-heating pyrolysis. The intrinsic kinetic parameters for oxidation of the residual organic carbon were determined by a least squares fit of the measured and calculated fraction reacted, as shown in Fig. 4 for experiments at 384 and 474°C. The measured fraction reacted was obtained by integrating the net rates of evolution of CO_2 and CO at constant reactor temperature. It is important to limit the experimental temperature to less than approximately 475°C in order to preclude CO_2 contribution from carbonate-capture of SO_2 that is being evolved from sulfide oxidation. A single reaction that is first-order with respect to organic carbon did not give a satisfactory fit to the experimental data. A single second-order reaction, however, was found to fit the experimental data very well. The second-order reaction rate coefficient, determined from the Arrhenius plot of eight experimental runs at constant temperatures ranging from 384 to 474°C, is

$$k = 1.33 \exp(-9780/T)\ s^{-1}\ Pa^{-1}$$

Two simultaneous first-order reactions fit the integrated experimental data quite well, but not as well as a single second-order reaction.

Previous work at this laboratory also indicated a second-order reaction for char combustion, but at an appreciably faster apparent rate than the above. In those earlier experiments, however, only CO_2 evolution was measured and temperatures up to 555°C were used. Both of these factors would cause the apparent char combustion rate to be incorrectly high (due to

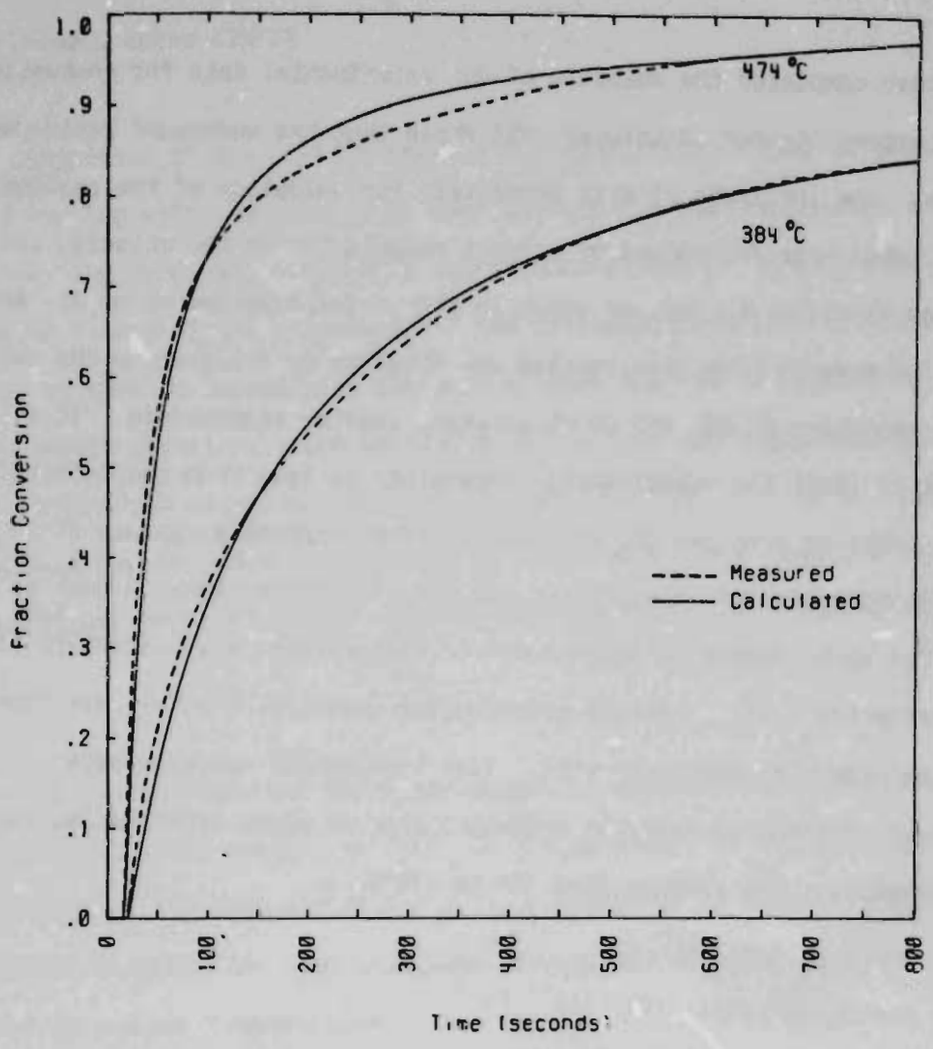

Figure 4. Fraction of residual organic carbon oxidized.

significant early release of CO_2 from carbonate-capture of SO_2 at temperatures above 475°C).

Comparison of the present results for combustion of char prepared by rapid heating with the results of Sohn and Kim for char combustion after slow-heating pyrolysis indicate a significant effect of heating rate. In order to make a direct comparison of the intrinsic kinetics for these two chars, we have re-interpreted the data of Sohn and Kim in terms of a second-order reaction, which was found to fit their data approximately as well as a first-order reaction. The comparisons are shown in Fig. 5. The rapid-heating char appears to be two to three times more reactive than the slow-heating char. We are continuing to investigate the effect of heating rate.

Bearing in mind that the temperatures of interest for combustion of retorted oil shale are in the range of 500 to 650°C, or higher, Fig. 5 dramatically illustrates that our present knowledge of the applicable intrinsic kinetics for char oxidation depend upon extrapolation from appreciably lower temperatures. This may not be quite as dangerous as it would appear from Fig. 5, however, since at the upper part of this temperature range the rate of char combustion will be controlled more by the effective diffusivity of oxygen into the shale particle than by the intrinsic oxidation kinetics.

III. GENERIC PYROLYSIS MODELING

Reactions of complex organic molecules can be interpreted by allowing a Gaussian distribution for the activation energy. One of the consequences of

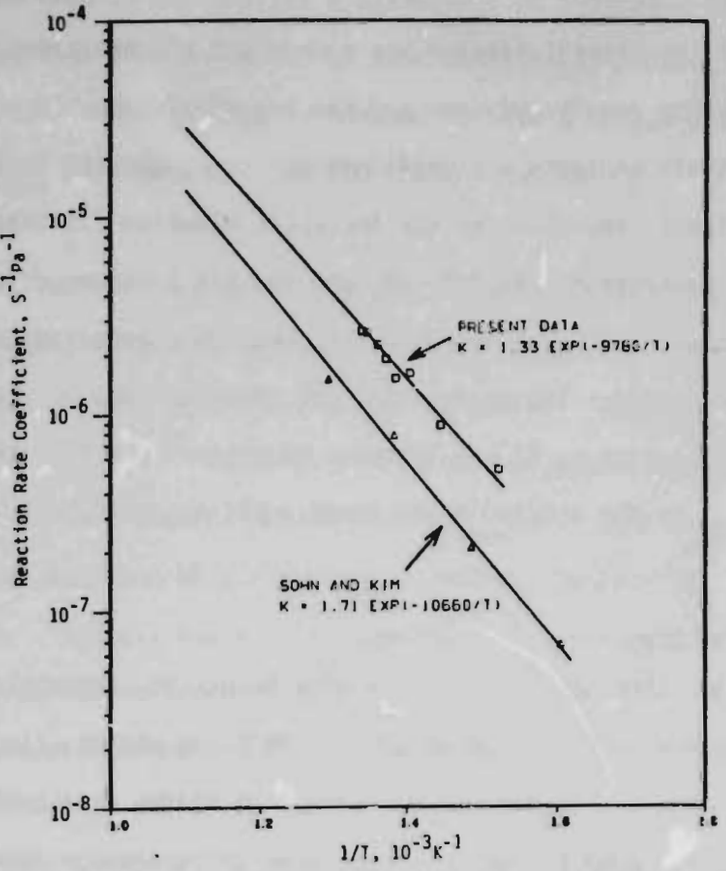

Figure 5. Arrhenius plot for char oxidation, assuming a 2nd-order reaction with respect to residual organic carbon. The original data of Sohn and Kim were reinterpreted in terms of a 2nd-order reaction.

doing this is that the kinetics of the reaction are then influenced by the past history of the reactants. For example, the temperature (T_{max}) at which the reaction rate is maximum for a given heating rate will be a function of the fraction that is pre-reacted at some other heating rate. This is in contrast with a reaction that is assumed to have a single activation energy, for which T_{max} is independent of the reaction history.

We have modified our generic pyrolysis model, PYROL, to enable extreme changes in heating rate to be made in a given run. Then we determined T_{max} at a moderate heating rate of 10°C/min for various fractions pre-reacted at a very low heating rate of 10^{-9} °C/hr (typical of geologic heating rates in petroleum basins). Significant shifts in T_{max} were obtained, depending on the standard deviation of the activation energy distribution and the fraction pre-reacted. Figure 6 illustrates some typical normalized reaction rate profiles at a heating rate of 10°C/min for 0, 10, 50, and 90% pre-reacted at 10^{9} °C/hr, assuming that the standard deviation of the activation energy is 8%. Note that T_{max} shifts from 457°C at 10% or less pre-reacted to 487°C at 50% pre-reacted and to 550°C at 90% pre-reacted. Figure 7 summarizes the effects of the standard deviation ranging from 0 to 16% of the principal activation energy. This method, when used in conjunction with kinetic data for pyrolysis of Type II kerogen, will be useful in determining the maturity of samples taken from petroleum basins.

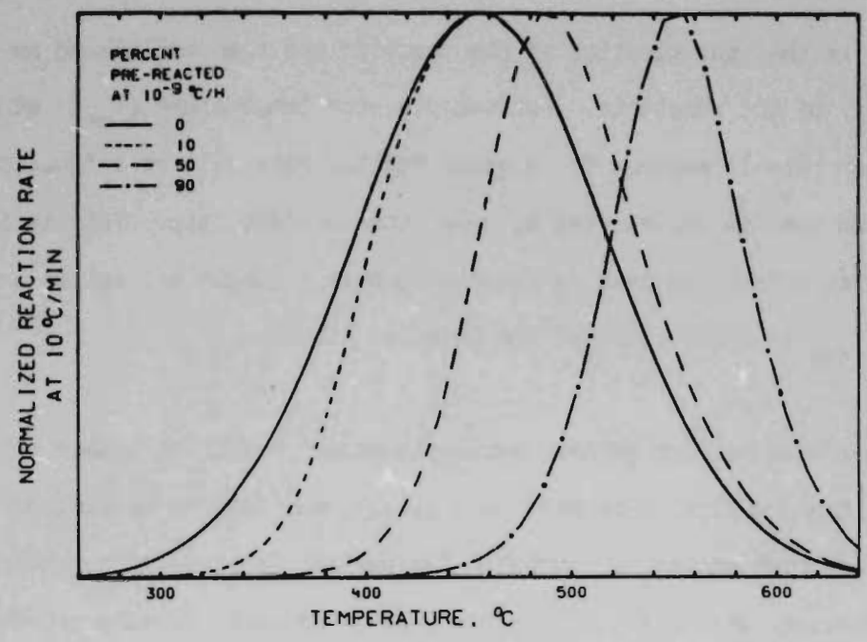

Figure 6. Shift of reaction rate profile at 10°C/min for 0, 10, 50, and 90% pre-reacted at 10-9°C/hour, assuming σ_E = 8%.

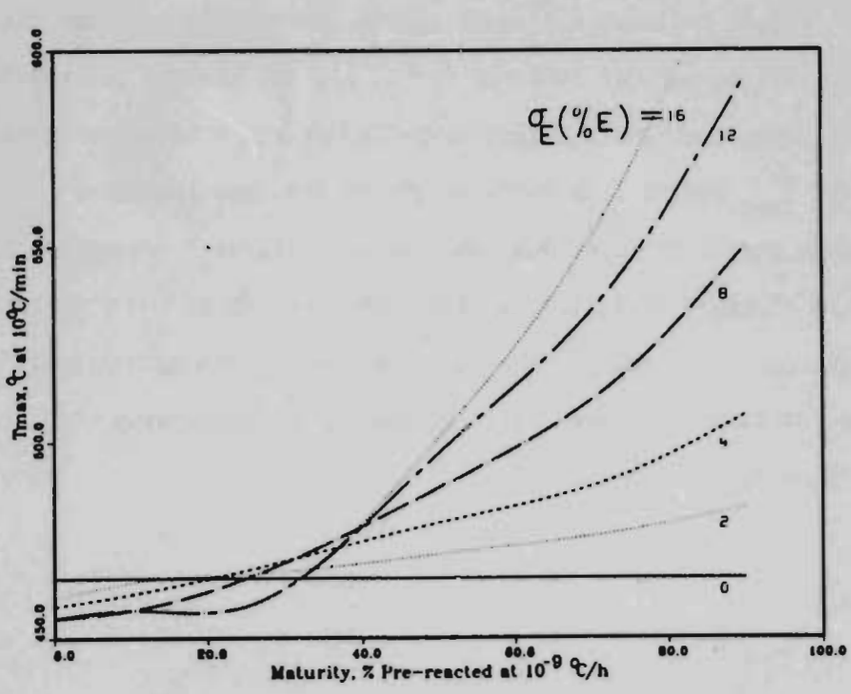

Figure 7. Tmax at 10°C/min as a function of maturity, for σ_E = 0 to 16% E.

END OF PAPER